

## Controlling chaos in a Lorenz-like system using feedback

G. Kociuba\* and N. R. Heckenberg

*Department of Physics, University of Queensland, St. Lucia, Queensland, Australia*

(Received 10 December 2002; revised manuscript received 24 July 2003; published 31 December 2003)

We demonstrate that the dynamics of an autonomous chaotic laser can be controlled to a periodic or steady state under self-synchronization. In general, past the chaos threshold the dependence of the laser output on feedback applied to the pump is submerged in the Lorenz-like chaotic pulsation. However there exist specific feedback delays that stabilize the chaos to periodic behavior or even steady state. The range of control depends critically on the feedback delay time and amplitude. Our experimental results are compared with the complex Lorenz equations which show good agreement.

DOI: 10.1103/PhysRevE.68.066212

PACS number(s): 05.45.-a

### I. INTRODUCTION

To observe chaos in nonlinear systems with two degrees of freedom one parameter must be modulated in order to create a third degree of freedom. Many laser chaos experiments are performed this way [1]. If a system already has three degrees of freedom, then it is possible for chaos to emerge without modulation and thus without an externally imposed time frame. The Lorenz-like chaos in the ammonia laser is an example of such autonomous chaos [2].

Dynamics of such chaotic systems have been studied extensively, both numerically [3], and experimentally [4–6]. Recently, there has been much effort put into control of chaos. This can be separated into two categories: feedback control (active control) and nonfeedback (passive) control. A number of feedback schemes can be used to control a chaotic system, such as control by occasional proportional feedback [7], control by synchronization [1], and the well-known Ott-Grebogi-Yorke (OGY) method. All these methods vary in complexity, and may be difficult to implement in a system with limited bandwidth. This is because the computation time to calculate detailed information about the system is significant. There are other feedback methods that do not require any computation, but instead rely on extracting a system variable and feeding that back into another variable or parameter. This control method is often called “feedback control” and is understood in the literature to mean subtractive feedback. That is, the control signal is expressed in the form  $F(t) = G(x(t) - x(t - \tau))$ , where  $\tau$  is the delay time, and  $G$  is some function with the condition that  $G(0) = 0$ . One example is control of a chaotic CO<sub>2</sub> laser by feedback of a variable which has been subtracted from its value at an earlier time [8].  $F(t)$  can be thought of as an error signal which tends to zero as the system approaches control, control meaning a periodic state where  $x(t) = x(t - \tau)$ . The advantage of this type of scheme is that no knowledge of the system other than the average pulsation period is required (control is only achieved for certain values of  $\tau$  in the vicinity of the average pulsation period). Experiments with subtractive feedback on the Lorenz-like ammonia laser showed that control to periodic and even steady state is possible [9]. The

feedback error signal was generated by analog subtraction using a coaxial delay line. When the laser was controlled to a periodic state, the feedback signal was itself periodic, so we can think of this as self-synchronization. It has also been shown that this type of laser operating above the chaos threshold could be synchronized to another chaotic system via the pump [6]. Here we make a detailed theoretical analysis of the subtractive feedback system to elucidate the range of conditions under which control is possible. In an attempt to further simplify the control of chaos we have examined the possibility of avoiding the subtraction process in the generation of the feedback error signal. Now if  $F(t) = G(x(t))$  then  $F(t)$  is nonzero in general. This type of feedback has been investigated and is known to destabilize a system in general [10]. The advantage would be that no subtraction of delayed signals would be required. This type of control was observed in a loss modulated CO<sub>2</sub> laser [11,12] where negative feedback of subharmonic components extracted from the intensity signal was applied. This was achieved using a logarithmic amplifier followed by a “washout filter.” Here we numerically investigate control without, and with, a low and high pass filter, which is simpler than the washout filter method.

### II. NUMERICS

The Lorenz model is used to describe the dynamics of an ideal two level atom interacting with a traveling wave in a ring resonator. Although the atoms are pumped like a three level system, it can be shown that the three level system can reduce to a two level system to a good approximation [13]. Our autonomous system has been shown to have a wide range of dynamics for various parameter ranges. Nearly all this behavior has been reproduced using the Lorenz equations or the complex Lorenz equations [14]. The complex equations take into account the fact that in the case of laser systems the cavity frequency is detuned from the atomic resonance in general. We use the complex Lorenz equations in our simulations of delayed feedback on a chaotic system. The complex Lorenz equations are

$$\dot{E} = -[(1 + i\delta)E - \lambda P],$$

$$\dot{P} = -(1/\sigma)[(1 - i\delta)P - ED], \quad (1)$$

$$\dot{D} = (\beta/\sigma)[1 - D + f(t) - 1/2(E^*P + P^*E)],$$

\*Electronic address: kociuba@physics.uq.edu.au

where

$$\sigma = \kappa / \gamma_{\perp}, \quad \beta = \gamma_{\parallel} / \gamma_{\perp}.$$

$E$ ,  $P$ , and  $D$  are the electric field, polarization, and inversion, respectively;  $\lambda$  is the average pump level,  $f(t)$  is the modulation applied to the pump;  $\delta$  is the detuning of the cavity resonance relative to the atomic line center;  $\kappa$ ,  $\gamma_{\parallel}$ , and  $\gamma_{\perp}$  are the cavity, polarization, and inversion decay rates, respectively. In all our simulations the parameters are  $\sigma = 1.5$ ,  $\beta = 0.25$ ,  $\delta = 0.2$ , and  $\lambda = 46$ . For chaos to occur the relation between the decay rates must be  $\kappa > \gamma_{\parallel} + \gamma_{\perp}$ . This is known as the bad cavity condition since a lossy cavity is required.

Variations in the pump power directly affect the population inversion so the feedback term appears as  $f(t)$ . We investigate two cases of feedback, the first being of the form of subtractive feedback [15]  $f(t) = A[I(t) - I(t - \tau)]$  where  $I(t) = E(t)E^*(t)$  represents the laser intensity, and  $A$  is the feedback amplitude. This type of feedback was experimentally implemented by driving an acousto-optic modulator (AOM) with a signal generated using a coaxial cable delay line to perform the subtraction [9]. To compare these results with our numerical results, we introduce an additional delay in the feedback loop of our model to account for the propagation delay  $T$  within the AOM used to convert the error signal into a modulation of the pump power. For the second case of nonsubtractive feedback, we dispense with the subtraction step and set the feedback to be  $f(t) = AI(t - T)$  and investigate the amplitude-feedback delay parameter space. In both these feedback cases the system is operating well above the chaos threshold  $\lambda_{th}$  so that the average pump level  $\lambda$  is chosen such that  $\inf(\lambda + f(t)) > \lambda_{th}$ . In all our calculations time is scaled [16] as  $\kappa t$  which is dimensionless since  $\kappa$  represents the cavity decay rate, hence the feedback variables  $T$  and  $\tau$  are also dimensionless.

### A. Control by subtractive feedback

As explained above, in all our experiments there was an additional delay  $T$  within the AOM, so we define the feedback term to be

$$f(t) = A[I(t - T) - I(t - (T + \tau))]. \quad (2)$$

The difference delay  $\tau$  is the time between the two measurements of output intensity, the difference between which constitutes the error signal. The feedback delay is defined as the time  $T$  for the feedback signal to enter back into the system. We integrate the complex Lorenz equations using this feedback term, and for different pairs of parameters  $\tau$ ,  $T$  and amplitude  $A$ , construct the time series  $I(t)$  associated with each of the parameters. Periodic solutions were identified from the time series and the periodicity of  $I(t)$  was determined ignoring the initial transient behavior before long term dynamics took over. The period of the time trace was plotted on the difference delay–feedback delay parameter space, for periods up to 6. Where no period was identified, the plot was left blank. The first result was calculated using a very weak feedback amplitude 0.0004 and the plot is shown in Fig. 1.

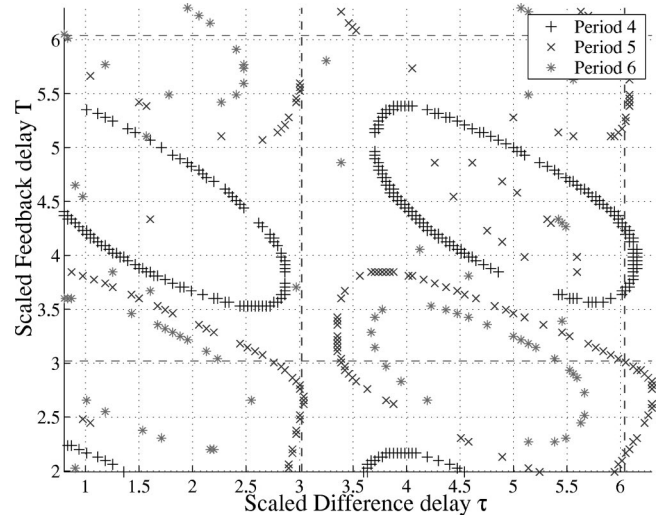


FIG. 1. Control to various periods by subtractive feedback of maximum amplitude of 0.04% of the pump. The difference delay  $\tau$  and the feedback delay  $T$  are both dimensionless, see text for details.

Since the intensity pulsations range between 80 and 120 units, this sets the maximum feedback amplitude to be about 0.04% of the average pump power. The average scaled pulsation period is 3.08. Only periods greater than 3 exist for very weak feedback as is evident in Fig. 1. If the feedback amplitude is increased to 0.001, equivalent to 10% of the average pump power, we find this increases the number of periodic states and leads to the existence of period 0—the steady state. This is shown in Fig. 2, where the dashed line indicates the average scaled pulsation period for the chaotic system without feedback (3.08). Many of the features in the weak feedback case in Fig. 1 are evident in Fig. 2, such as the rings of period 4 in parameter space. In the stronger feedback case, these rings have been distorted and the positions shifted slightly. These rings contain regions of control

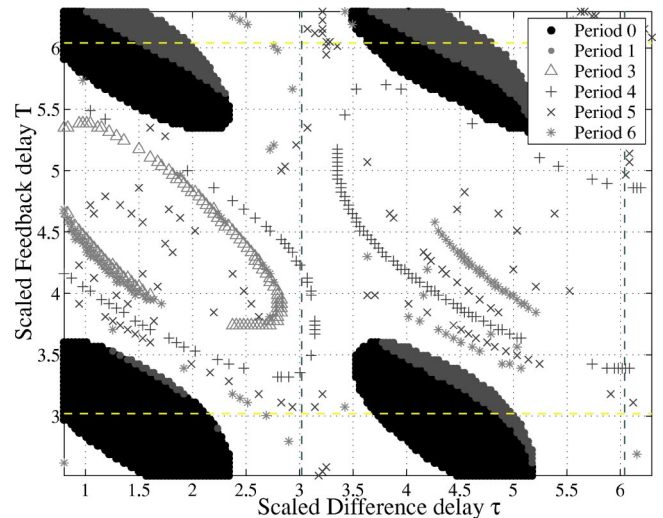


FIG. 2. Control to various periods by subtractive feedback of maximum amplitude 10% of the pump. The difference delay is  $\tau$ , and the feedback delay is  $T$ .

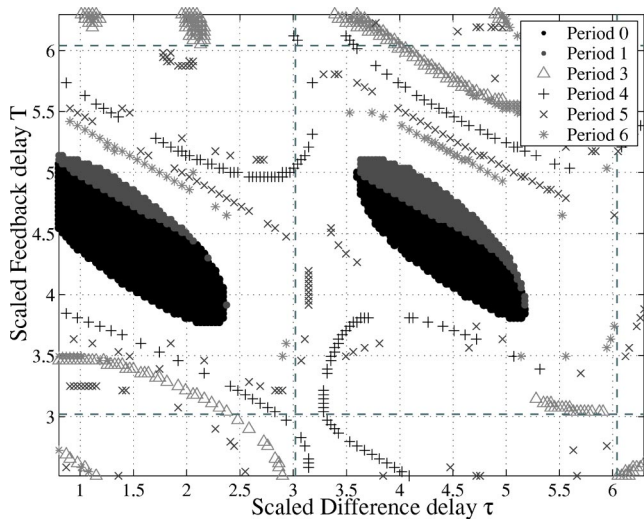


FIG. 3. Control to various periods by subtractive feedback of maximum amplitude 10% of the pump. The difference delay is  $\tau$ , and the feedback delay is  $T$ . The error signal has been inverted with respect to Fig. 2.

to less than period 4 where period 0 dominates. As might be expected, islands of control exist at multiples of the average pulsation period along the feedback delay axis. The same applies for the difference delay axis. If we leave the feedback amplitude at 0.001 but change the sign of the feedback to negative, the result is shown in Fig. 3. There are similar structures here as in the previous figure except that the islands are displaced half an average pulsation period upwards. This can be understood by considering the change of sign of the feedback term to be equivalent to a phase shift of half a period. These well defined islands of stability are destroyed if the feedback amplitude is too large. We increased the feedback amplitude to 0.006 which would correspond to an average of 60% of the average pump power. The result is shown in Fig. 4. Since the feedback amplitude modulation is so large it is no longer perturbative and the system is no longer Lorenz like. Figure 4 shows there are now islands of control which are not at multiples of the average pulsation period of the unperturbed system in either the difference delay axis or the feedback delay axis. The size of the period 0 islands are significantly smaller in the strong feedback case compared to the moderate feedback case as in Fig. 2. One would expect the islands to be smaller since if the system is not very close to the periodic state, then the large feedback amplitude drives the system quickly away from the periodic state. Previous experiments on the ammonia laser [9] showed that the laser was controlled to period 0 when the feedback amplitude was 3% and 7%. The difference delay  $\tau$  used was about one laser pulse period. Control to period 1, 2, 4, 6 was observed at 5% modulation depth. Numerically, we found control to period 0, 1, 3, 4, 5, 6 with a modulation depth of 10% for the second multiple of the average pulsation period as well as the first multiple. We did not find any period 2 at this amplitude. This could be due to the fact that numerically we calculated the period of the intensity traces which contained about 1000 pulsations. The experiments have the limitation that only about 70 pulses during control could be re-

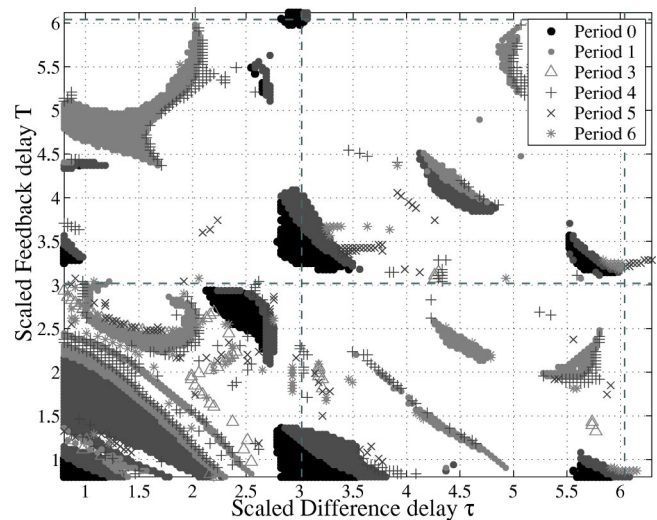


FIG. 4. Control to various periods by subtractive feedback of maximum amplitude of 60% of the pump. The difference delay is  $\tau$ , and the feedback delay is  $T$ .

corded. Thus it is possible that what appeared to be period 2 was actually a long transient which approaches period 1. This is always a problem with any finite time series since one cannot be sure whether the dynamics in a finite time series is permanent or transient.

The islands of stability have a definite preferred orientation, in particular the period 0 islands all have a slope of  $-\frac{1}{2}$ . This can be understood the following way. Period 0 occurs after the oscillation is completely damped so just before it is extinguished it is a sinusoid to a very good approximation. So we can write the signal as  $f(t) = a \sin(\omega t)$  and the delayed signal will be  $f(t + \phi) = a \sin(\omega(t + \phi))$ , where  $\phi$  is the phase difference between the two signals due to the subtraction time  $\tau$  so  $\phi = \tau\omega$ . Since  $f(t) - f(t + \phi) = -2a \sin(\omega\phi/2) \cos(\omega(t + \phi/2))$ , the generated difference signal has an effective delay equal to half the delay  $\tau$  within the control island which can be compensated by an equal but opposite change in the feedback delay  $T$ .

We now look at the stability of the fixed points of the nonlinear system to gain some insight into the mechanism of control. The eigenvalues of the feedback system cannot be obtained analytically since the determinant of the Jacobian is a transcendental function, so this can only be solved numerically. There are an infinite number of complex solutions to this type of equation in general, and the system will be stable if all the eigenvalues are negative. We search the same parameter space as in Fig. 2 and set  $A = 0.001$  and plot (Fig. 5) whenever all the eigenvalues of the determinant of the Jacobian are less than or equal to zero. Without the feedback [ $f(t) = 0$  in Eq. (1)] the eigenvalues of these fixed points are positive. It is clear that the position of the islands of control to period 0 and period 1 are contained within the islands in Fig. 5. This shows that the eigenvalues of the fixed points of the system are all negative during control to period 0 and period 1. Control to a periodic state by stabilizing an existing unstable periodic orbit of a chaotic attractor has previously

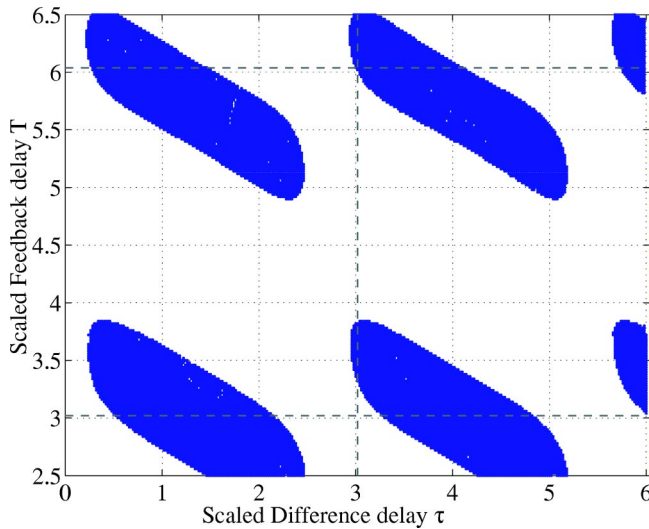


FIG. 5. Islands represent the nonpositive Lyapunov spectrum of Eq. (1) for the feedback parameter  $A=0.001$ . The difference delay is  $\tau$ , and the feedback delay is  $T$ .

been demonstrated experimentally and theoretically as discussed in the Introduction. These methods of control rely on the state of the system having a reasonable probability of visiting the desired unstable periodic orbit where a control mechanism can take full effect. This is not the case for period 0 since the state never visits the unstable fixed point [17]. We overcome this by applying the feedback. This changes the stability of the unstable fixed points, allowing an initially inaccessible region of phase space to be visited for certain values of feedback parameters as shown in Fig. 5.

In previous feedback experiments [9] and in our experimental results following this section, the feedback signal to the laser system is ac coupled. This will only give a nonzero final error signal if the unfiltered error signal is varying with time, and a constant unfiltered signal will appear as zero final error signal. To check what effect this might have, we include this effect in our model by applying a high pass and a low pass filter to  $f(t)$  and using this modified  $f(t)$  as the feedback signal in the differential equations. The high pass filter models the ac coupling while we also include a low pass filter to model the finite bandwidth of the AOM. We apply this procedure to the subtractive feedback case for six different values of low pass cutoff angular frequencies 6, 2, 1, 0.85, 0.75, and 0.5 where in each case the high pass cutoff was set to 0.01. The result for the high cut off angular frequency of 1 is shown in Fig. 6. The characteristic scaled pulsation period is 3.08 (hence the scaled angular frequency is  $\approx 2$ ), where time has been scaled to the parameter  $\kappa$ . The cutoff frequency 6 is  $\approx$  three times the average pulsation frequency and we found that this results in only a slight decrease of the amplitude of the fundamental frequency component allowing control to proceed. As the cutoff frequency decreases, there is a greater attenuation of the fundamental frequency which gets fed back into the equations. This results in an effective lower modulation amplitude at the fundamental frequency and therefore the range of control becomes narrower. This is evident by comparing Fig. 6 to Fig.

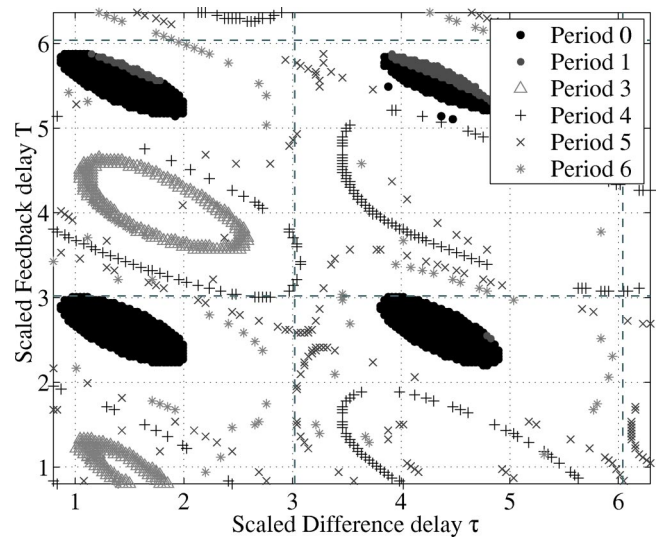


FIG. 6. Control to various periods by subtractive feedback for a high and low pass cutoff scaled frequencies  $\omega$  are 1 and 0.01, respectively. The scaled (dimensionless) average pulsation frequency  $\omega_0$  is 2.

2 (which is unfiltered, but is found to look similar to a cut off frequency of 6) where the islands of control retain their orientation but decrease in size. All the period 0 islands were found to have been extinguished for a cutoff frequency of 0.5, and the lowest period was 4. These results show that the effects of ac coupling and the limited bandwidth of the AOM can reasonably be neglected in the theoretical modeling. There is only a significant difference when the bandwidth of the feedback signal is equal to or less than the characteristic frequency of the system, and this just causes the control islands to shrink and get destroyed if the bandwidth is much less than the characteristic frequency.

### B. Control by nonsubtractive feedback

We now simplify the feedback term so that there is no subtraction and simply take  $f(t)=AI(t-T)$ . As before we integrate the complex Lorenz equations using this feedback term, and for different pairs of parameters  $T$  and amplitude  $A$ , construct the time series  $I(t)$  associated with each of the parameters. The periodicity of  $I(t)$  was calculated the same way and a map of the results as a function of delay and feedback amplitude was constructed as shown in Fig. 7. To save time, relatively larger steps in the feedback amplitude  $A$  were used. Again the scaled average pulsation period of the unperturbed system is 3.08 as indicated by the dashed line. Period 0 dominates the regions near multiples of the scaled average pulsation period, 3.08 and 6.16, which first appear at a feedback amplitude of  $1.1 \times 10^{-3}$  corresponding to about 11% modulation depth. As this amplitude increases more different period numbers emerge. The numerical results in Fig. 7 show that control to period 1 occurs only on the right hand side of the large period 0 block. This segment of period 0 begins at slightly more than the average pulsation period of the unperturbed system. This is the only region we can explore experimentally since there are delays in the acousto-optic modulator which cannot be removed.

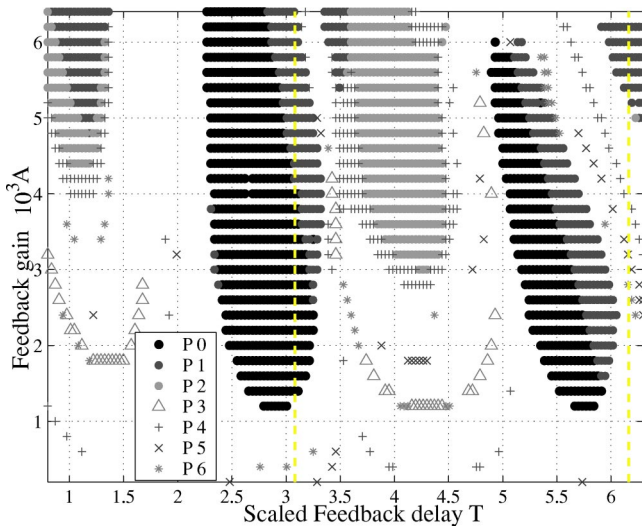


FIG. 7. Control to various periods by nonsubtractive feedback as a function of the difference delay  $\tau$  and feedback amplitude  $A$ .

The eigenvalues of the Jacobian of Eq. (1) are calculated and regions where all eigenvalues are non-positive are delineated in Fig. 8. The period 0 and period 1 islands from Fig. 7 appear in a similar position to the islands in Fig. 8. This shows that the stabilization of the fixed points during control to period 0 and period 1 allows an initially inaccessible region of phase space to be reached.

Three measures are introduced to extract information about the dynamics during and near a control window. The periodicity is calculated as before, and the number of transient pulses before control was achieved is calculated and referred to as “transient pulses.” The difference between the number of cycles of output intensity and the feedback signal was calculated (which is related to the average frequency difference) then this difference is determined over the duration of the feedback. This measure is referred to as the “average phase difference.” Finally, “phase slips” are calculated

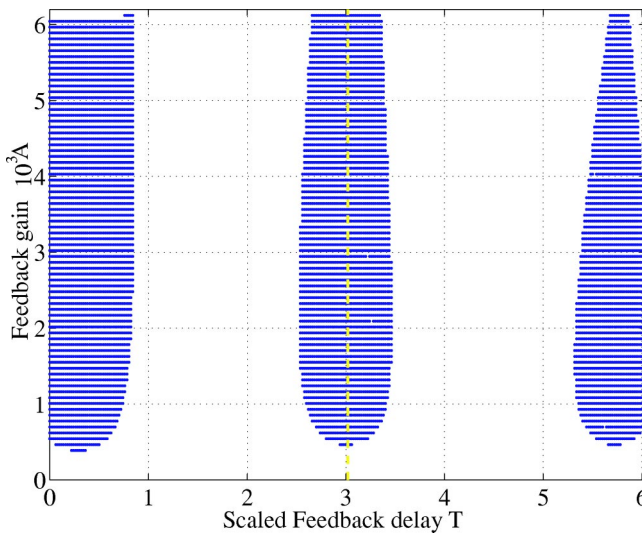


FIG. 8. Islands represent an all nonpositive Lyapunov spectrum of Eq. (1). The feedback delay is  $T$  and amplitude is  $A$ .

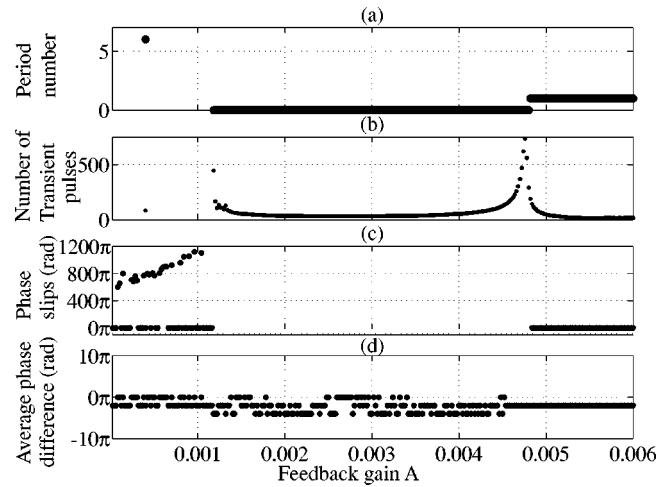


FIG. 9. The period number, number of transient pulses before control emerges, phase slips, and average phase difference, as a function of feedback amplitude are shown in (a), (b), (c), and (d), respectively.

by comparing each successive intensity peak time and feedback peak time keeping track of their relative orientation, and counting the number of times the sign of the difference between these peak times changes. This measure is used since there are situations where the average frequencies of two quantities are the same yet there may be an equal number of positive and negative phase slips which cannot be extracted from the average phase difference measure alone.

The feedback delay has been set to  $T=3$  which corresponds to a vertical line at  $T=3$  in Fig. 7, and the measures are calculated for the same range of amplitude points as Fig. 7, except the number of amplitude points was increased tenfold for higher resolution. The number of transient pulses before control emerged is shown in Fig. 9(b) indicating that the fastest rate of convergence to the periodic state is  $\approx$  in the center of the amplitude control window shown in Fig. 9(a). There is a period 6 orbit at  $A=0.0004$  which has a corresponding low number of transient pulses.

The average phase difference, which is related to the average frequency, is displayed in Fig. 9(d), and the difference is less than  $4\pi$  rad where the number of cycles is  $\approx 1000$ . This shows that the weakest form of generalized synchronization occurs for the whole amplitude range calculated for the fixed feedback delay of  $T=3$ . To determine which regions of the generalized synchronization states are phase locked, the number of phase slips was calculated and is shown in Fig. 9(c). There are generally few phase slips during the controlled state, indicating phase locking. Phase slips were not calculated for the amplitude range corresponding to period 0 as synchronization has no meaning at steady state.

There are some phase slips for  $A < 0.0011$  but this amounts to only 18% of the data points in this region giving a high synchronization ratio of 82%.

The measures used in this analysis show that generalized synchronization occurs for a wide range of feedback parameters, and perfect synchronization occurs before control emerges for  $0.0011 < A < 0.0013$ . The phase slip measures can show when a dynamical state is approaching the edge of

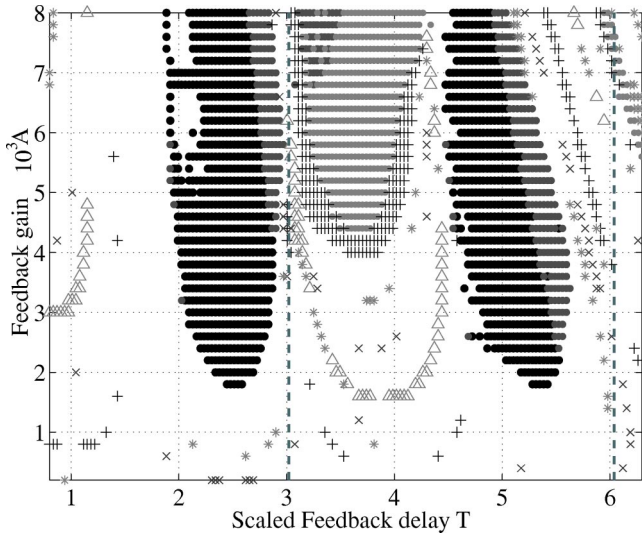


FIG. 10. Control to various periods by nonsubtractive feedback for a scaled cutoff angular frequency of 1. The low pass cutoff is 0.01.

an Arnold tongue which is not observed by comparing average frequencies, and quantifies the quality of the synchronized state.

We now modify the nonsubtractive feedback system by including filtering and the result for the cutoff angular frequency of 1 is shown in Fig. 10. Again as the low pass cutoff is decreased there is less modulation at the fundamental frequency so a greater feedback amplitude is required to compensate. This is evident in the figure as the islands of control move towards a higher amplitude of feedback as the cutoff is decreased. These results show that limiting the bandwidth of the error signal has the effect of raising the threshold for control and for a sufficiently large bandwidth the results are essentially the same as the unfiltered case.

III. EXPERIMENTAL

Our experimental system consists of a <sup>13</sup>CO<sub>2</sub> laser which optically pumps a <sup>15</sup>NH<sub>3</sub> ring laser through a vibration transition at 10.78 μm. The lasing occurs through a rotational transition at a wavelength 0.153 mm. We use a semi-confocal ring cavity as shown in Fig. 11 to achieve unidirectional lasing, where the backward traveling wave is chosen in preference to the forward wave because the ac Stark effect splits the gain line in the forward direction [18]. This allows us to use the Lorenz equations to describe the dynamics of our laser system [13]. The intensity of the backward wave in the ring laser is measured with a Schottky barrier diode B. This signal is monitored by a spectrum analyzer and recorded by a digital storage oscilloscope. In order to implement the non-subtractive feedback scheme a signal proportional to the laser output has to be fed back to modulate the pump power. The signal  $I(t)$  is therefore fed into a buffering amplifier, amplified, then applied to the acousto-optic modulator. The finite acoustic velocity in the AOM creates a delay that could be varied by ≈ 20% of the fundamental pulsation period by adjusting the AOM’s position transverse to the CO<sub>2</sub> pump

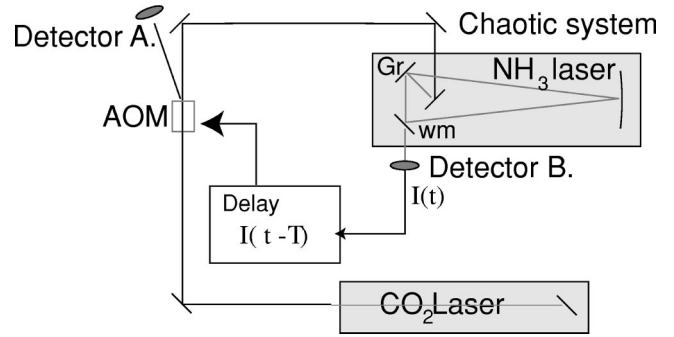


FIG. 11. Experimental schematic. Gr is a blazed grating at the pump wavelength which doubles as a mirror for the lasing wavelength. wm is a wire mesh used as an output coupler. The far-infrared (FIR) intensity output is measured, delayed, and applied to the AOM

beam. There is a second detector A which is used to monitor the pump dynamics. This signal is simultaneously recorded with detector B onto a digital storage oscilloscope.

IV. EXPERIMENTAL RESULTS

The delay time  $T$  was adjusted so that this corresponded to the average pulsation period of the laser. Control to period 1 was observed as shown in Fig. 12. Here the average feedback amplitude was 5%. Before the feedback control was turned on (at  $t=1.2$  ms) the laser produced Lorenz-like chaos. Initially the control signal caused the Lorenz-like pulsations to break into transient pulses before the system settled to period 1 pulsations, and the feedback signal was also periodic. The phase difference between the feedback signal and the intensity output was locked only during the controlled state as expected. The smallest feedback delay which could be achieved in the experiment was about twice the average pulsation period of the unperturbed system so that we could not explore  $\tau < 6.0$  in Fig. 7.

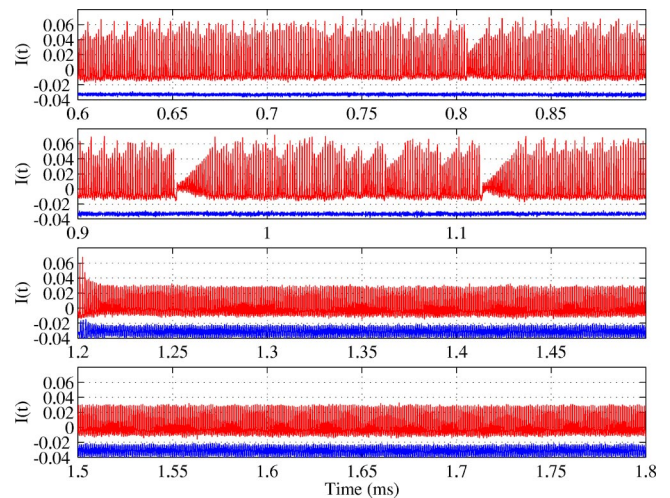


FIG. 12. Control to period 1 using nonsubtractive feedback of the FIR laser with  $A \approx 0.05$ . The average pulsation period before and during control is 1.179 μs and 0.9747 μs, respectively. The intensity is in arbitrary units.

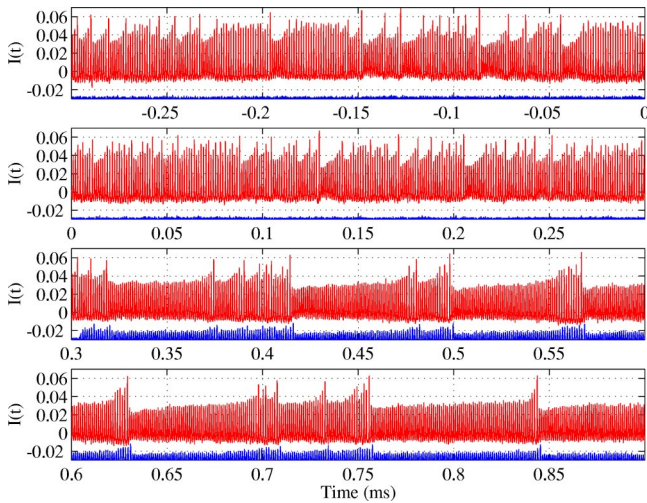


FIG. 13. Synchronization by nonsubtractive feedback. Average pulsation period before feedback and during feedback are  $1.1933 \mu\text{s}$  and  $1.068 \mu\text{s}$ , respectively. There are no phase slips when the non subtractive feedback is turned on. The intensity is in arbitrary units.

We also find that when the sign of the feedback is reversed, control can still be achieved by adjusting the delay of the feedback (not shown since it looks the same as nonreversed feedback).

We also found that outside the range where control was achieved, the initially chaotic intensity can be synchronized so that the output and feedback is fully phase locked, and the time series is shown in Fig. 13. It appears that a different type of chaos is produced during feedback. This resembles Lorenz-like chaos operating closer to the chaos threshold (from above) compared to the unperturbed system due to the lengthening of the spirals. To check for phase slips a histogram is calculated for the time difference between the FIR intensity peaks and the feedback signal, and the result is shown in Fig. 14. During synchronization there is a significant lag between the FIR intensity, and the feedback signal, and all time differences are within the average pulsation period  $T = 1.068$ .

The histogram contains two peaks where the larger peak corresponds to the start of the spiral, and the smaller to the end of the spiral which is preceded by  $\approx$  ten cycles with a significantly larger period than the average. The average pulsation period decreases with increasing pump strength when no feedback is applied, so the feedback has increased the period during the last few cycles of the spiral despite the fact that the average energy of the pump during that region is slightly higher than at the start of the FIR spiral.

These results show that control to period 1 can be achieved by choosing an appropriate delay time. Synchronization can also be achieved, which can be used to create a modified chaos which has a higher bandwidth than the unperturbed system which is phase locked to the delayed signal.

## V. CONCLUSION

We numerically investigated control of Lorenz-like chaos to various periodic states including period 0 using two feed-

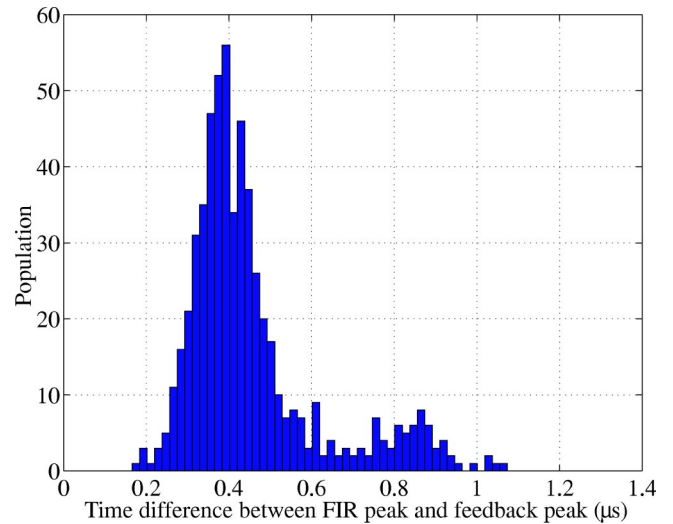


FIG. 14. This shows the frequency of occurrence for the time difference between the FIR intensity peaks, and the associated pump fluctuation peaks, corresponding to Fig. 13. The average pulsation period is  $1.068 \mu\text{s}$ . Peak detection error ranges from  $0.05$  to  $0.1 \mu\text{s}$ .

back control methods. The first case was subtractive feedback of intensity including loop delay. We found that for a small amplitude control to periods greater than 3 existed. At moderate feedback amplitude, control to period 0, 1, 3, 4, 5, and 6 emerged where large islands of period 0 dominate the difference delay–feedback delay parameter space. These islands are separated by the average pulsation period of the system. They can be shifted half a period by inverting the feedback signal. We showed that islands of period 0 and period 1 correspond to a nonpositive set of eigenvalues of the chaotic system with feedback emphasizing that a nonperturbative picture is necessary to understand the full range of opportunities for control, which are not limited to preexisting unstable periodic orbits. We then examined the effect of applying an ac filter to the feedback signal and varied the bandwidth before feeding it into the chaotic equations. Control is still possible even if the high pass cutoff frequency was slightly less than the characteristic frequency of the system. The results are in good agreement with previously published experimental results.

The second feedback case consisted of a simpler subtraction-free feedback with only a loop delay. We found control to the same periodic cycle numbers as in the subtractive case at the same feedback amplitude, and with the addition of period 2. The period 0 and period 1 islands dominate the feedback delay–amplitude parameter space. These islands corresponds to the fixed points of the feedback system containing no positive eigenvalues. Phase slips were calculated indicating not only perfect synchronization just before (and during) control, but also for very low feedback amplitudes. Modifying the feedback signal by applying the same a.c. filtering and finite bandwidth as in the subtractive feedback case, we find that this has the effect of raising the threshold amplitude for control as the bandwidth approaches the characteristic frequency of the system. Experimentally we were able to control a chaotic Lorenz-like laser to period

1 by this nonsubtractive method and found control to period 1 but were prevented from demonstrating period 0 by time delays in the AOM. Phase synchronization was experimentally observed for a relatively large frequency mismatch of 11.7% between the initial and final average pulsation frequencies.

Overall, the concordance of experimental and theoretical

results confirms that control of a strongly chaotic system can be achieved by controlling a single parameter using an error signal based on a single variable, without any computations. Further, the system can be controlled not only to periodic states but also to the technically more useful steady state even though this region of phase space is inaccessible in the original system.

- 
- [1] R. Roy and K.S. Thornburg, Jr., *Phys. Rev. Lett.* **72**, 2009 (1994).
- [2] C. Weiss and W. Klische, *Opt. Commun.* **51**, 47 (1984).
- [3] J.-P. Eckmann, and D. Ruelle, *Rev. Mod. Phys.* **57**, 617 (1985).
- [4] S. Bielawski, D. Derozier, and P. Glorieux, *Phys. Rev. A* **47**, R2492 (1993).
- [5] W.X. Ding, H.Q. She, W. Huang, and C.X. Xu, *Phys. Rev. Lett.* **72**, 96 (1994).
- [6] D.Y. Tang, R. Dykstra, M. Hamilton, and N.R. Heckenberg, *Phys. Rev. E* **57**, 3649 (1998).
- [7] R. Roy, J.T.W. Murphy, T.D. Maier, and Z. Gills, *Phys. Rev. Lett.* **68**, 1259 (1992).
- [8] S. Bielawski, D. Derozier, and P. Glorieux, *Phys. Rev. E* **49**, R971 (1994).
- [9] R. Dykstra, D.Y. Tang, and N.R. Heckenberg, *Phys. Rev. E* **57**, 6596 (1998).
- [10] G. Huyet, J.K. White, A.J. Kent, S.P. Hegarty, J.V. Moloney, and J.G. McInerney, *Phys. Rev. A* **60**, 1534 (1999).
- [11] R. Meucci, M. Ciofini, and R. Abbate, *Phys. Rev. E* **53**, R5537 (1996).
- [12] M. Ciofini, A. Labate, and R. Meucci, *Phys. Lett. A* **227**, 31 (1997).
- [13] R. Gilmore, R. Vilaseca, R. Corbalan, and E. Roldan, *Phys. Rev. E* **55**, 2479 (1997).
- [14] C. Weiss, R. Vilaseca, N. Abraham, R. Corbalan, E. Roldan, and G. de Valcarcel, *Appl. Phys. B: Lasers Opt.* **B61**, 223 (1995).
- [15] K. Pyragas and A. Tamasevicius, *Phys. Lett. A* **180**, 99 (1993).
- [16] G. Kociuba and N.R. Heckenberg, *Phys. Rev. E* **66**, 026205 (2002).
- [17] R. Dykstra, J.T. Malos, N.R. Heckenberg, and R.G. McDuff, *Phys. Rev. A* **56**, 3180 (1997).
- [18] G. Willenberg, J. Heppner, and G. Schinn, *IEEE J. Quantum Electron.* **QE-18**, 2060 (1982).